

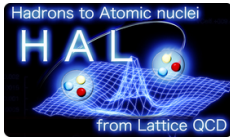
Baryon-baryon interaction of strangeness $S = -1$ sector

Hidekatsu Nemura*[†]

Department of Physics, Tohoku University, Sendai, 980-8578, Japan

E-mail: nemura.hidekatsu.gb@u.tsukuba.ac.jp

for HAL QCD Collaboration



We present our recent studies on hyperon-nucleon (YN) interactions in the strangeness $S = -1$ that $p\Lambda, \Sigma^0 p$ and $\Sigma^+ n$, by extracting corresponding potentials through Nambu-Bethe-Salpeter wave functions. We calculate ΛN and ΣN potentials in the isospin $I = 3/2$ channel, using the $N_f = 2 + 1$ gauge configurations generated by PACS-CS collaboration and employing an improved method to obtain potentials in lattice QCD simulations. For the 1S_0 channel, the central $\Sigma N(I = 3/2, ^1S_0)$ potential and the central $\Lambda N(^1S_0)$ potential are found to be very similar. In the spin triplet ($^3S_1 - ^3D_1$) channels, the central $\Lambda N(^3S_1 - ^3D_1)$ potential is attractive while the central $\Sigma N(I = 3/2, ^3S_1 - ^3D_1)$ potentials is repulsive. Tensor potentials, on the other hand, are rather weak in the diagonal part of both ΛN and $\Sigma N(I = 3/2)$ systems.

The XXIX International Symposium on Lattice Field Theory - Lattice 2011

July 10-16, 2011

Squaw Valley, Lake Tahoe, California

*Speaker.

[†]Present address: Center of Computational Sciences, University of Tsukuba, Tsukuba, Ibaraki, 305-8577, Japan

1. Introduction

The Λ -nucleon (ΛN) and the Σ -hyperon (ΣN) interactions are one of the basic inputs to study the hypernuclear systems. in which hyperons (or strange quarks) are embedded in normal nuclear systems as ‘‘impurities’’ [1]. For example, from studies of few-body systems for s -shell Λ -hypernuclei, it has been pointed out that a coupled-channel $\Lambda N - \Sigma N$ interaction plays a significant role to make a hypernucleus being bounded.[2]. On the other hand, no Σ -hypernuclei have been observed except for four-body Σ -hypernucleus (${}^4_{\Sigma}\text{He}$), and furthermore a recent experimental study suggests that Σ -nucleus interaction is repulsive. Such informations are useful to study properties of hyperonic matters inside the neutron stars [3], though a hyperonic equations of state (EOS) employed in such a study may contradict a recent observation of a massive neutron star heavier than $2M_{\odot}$ [4]. Despite their importance, present phenomenological ΛN and ΣN interactions have still large uncertainties since direct ΛN and ΣN scattering experiments are either difficult or impossible due to the short life-time of hyperons.

Recently, a new approach has been proposed lattice QCD to study not only the NN interaction but also various baryonic interactions including the H-dibaryon system [5, 6, 7, 8, 9, 10, 11], and the method is recently extended to systems in inelastic channels [12, 13]. This method has been applied also to study various interactions other than baryon-baryon interactions [14, 15]. In this approach, the interparticle potential can be directly extracted in lattice QCD through the Nambu-Bethe-Salpeter (NBS) wave function, and observables such as the phase shift and the binding energy can be calculated by using the resultant potentials. The purpose of this report is to present our recent calculations of the ΛN potentials as well as the $\Sigma N(I = 3/2)$ potentials using full QCD gauge configurations. Several earlier results had already been reported at LATTICE 2008[16] and LATTICE 2009[17]. This report is the latest version of those reports, which includes several new results: (i) $\Sigma N(I = 3/2)$ potentials are studied. (ii) An improved method is employed to extract potentials more precisely [18].

2. Improved extraction of potentials

In the HAL QCD scheme, the non-local but energy-independent potential is defined by the Schrödinger equation as

$$(\vec{\nabla}^2 + k^2) \phi(\vec{r}) = 2\mu \int d^3r' U(\vec{r}, \vec{r}') \phi(\vec{r}'), \quad (2.1)$$

where $\phi(\vec{r})$ is the equal-time NBS wave function of two-baryon system (B_1, B_2), $\mu = m_{B_1} m_{B_2} / (m_{B_1} + m_{B_2})$ and k^2 are the reduced mass of the (B_1, B_2) system and the square of asymptotic momentum in the center-of-mass frame, respectively. In practice, the nonlocal potential is expanded in terms of the velocity(derivative) as [19], $U(\vec{r}, \vec{r}') = V_{B_1 B_2}(\vec{r}, \vec{\nabla}) \delta(\vec{r} - \vec{r}')$. The potential V may have an antisymmetric spin-orbit term when two baryons are not identical. For example, the ΛN potential is given by

$$V_{\Lambda N} = V_0(r) + V_{\sigma}(r)(\vec{\sigma}_{\Lambda} \cdot \vec{\sigma}_N) + V_T(r)S_{12} + V_{LS}(r)(\vec{L} \cdot \vec{S}_+) + V_{ALS}(r)(\vec{L} \cdot \vec{S}_-) + O(\nabla^2), \quad (2.2)$$

where $S_{12} = 3(\vec{\sigma}_{\Lambda} \cdot \vec{n})(\vec{\sigma}_N \cdot \vec{n}) - \vec{\sigma}_{\Lambda} \cdot \vec{\sigma}_N$ is the tensor operator with $\vec{n} = \vec{r}/|\vec{r}|$, $\vec{S}_{\pm} = (\vec{\sigma}_N \pm \vec{\sigma}_{\Lambda})/2$ are symmetric (+) and antisymmetric (-) spin operators, $\vec{L} = -i\vec{r} \times \vec{\nabla}$ is the orbital angular momentum

operator. In the velocity expansion, $V_{0,\sigma,T}$ are the leading order (LO) potentials, denoted by V_{LO} , while $V_{\text{LS,ALS}}$ are of the next-to-leading-order (NLO). In this report, we consider the LO potentials only.

In lattice QCD simulations we first calculate the normalized four-point correlation function defined by

$$R_{\alpha\beta}^{(J,M)}(\vec{r}, t-t_0) = \sum_{\vec{X}} \left\langle 0 \left| B_{1,\alpha}(\vec{X} + \vec{r}, t) B_{2,\beta}(\vec{X}, t) \overline{\mathcal{J}_{B_3B_4}^{(J,M)}(t_0)} \right| 0 \right\rangle / \exp\{-(m_{B_1} + m_{B_2})(t-t_0)\}, \quad (2.3)$$

where the summation over \vec{X} selects states with zero total momentum. The $B_{1,\alpha}(x)$ and $B_{2,\beta}(y)$ denote the interpolating fields of the baryons such as

$$p = \varepsilon_{abc} (u_a C \gamma_5 d_b) u_c, \quad n = -\varepsilon_{abc} (u_a C \gamma_5 d_b) d_c, \quad (2.4)$$

$$\Sigma^+ = -\varepsilon_{abc} (u_a C \gamma_5 s_b) u_c, \quad \Sigma^0 = \frac{1}{\sqrt{2}} \varepsilon_{abc} \{ (d_a C \gamma_5 s_b) u_c + (u_a C \gamma_5 s_b) d_c \}, \quad (2.5)$$

$$\Lambda = \frac{1}{\sqrt{6}} \varepsilon_{abc} \{ (d_a C \gamma_5 s_b) u_c + (s_a C \gamma_5 u_b) d_c - 2 (u_a C \gamma_5 d_b) s_c \}, \quad (2.6)$$

and $\overline{\mathcal{J}_{B_3B_4}^{(J,M)}(t_0)} = \sum_{\alpha'\beta'} P_{\alpha'\beta'}^{(J,M)} \overline{B_{3,\alpha'}(t_0) B_{4,\beta'}(t_0)}$ is a source operator which creates $B_3 B_4$ states with the total angular momentum J, M . This normalized four-point function can be expressed as

$$R_{\alpha\beta}^{(J,M)}(\vec{r}, t-t_0) = \sum_n A_n \sum_{\vec{X}} \left\langle 0 \left| B_{1,\alpha}(\vec{X} + \vec{r}, t) B_{2,\beta}(\vec{X}, t) \right| E_n \right\rangle e^{-(E_n - m_{B_1} - m_{B_2})(t-t_0)}, \quad (2.7)$$

where E_n ($|E_n\rangle$) is the eigen-energy (eigen-state) of the six-quark system with the particular quantum number (i.e., J^π, M , strangeness S and isospin I), and $A_n = \sum_{\alpha'\beta'} P_{\alpha'\beta'}^{(J,M)} \langle E_n | \overline{B_{4,\beta'}} \overline{B_{3,\alpha'}} | 0 \rangle$.

Since $E_n - m_{B_1} - m_{B_2} = k^2/(2\mu) + O(k^4)$, we have[18]

$$\left(\frac{\nabla^2}{2\mu} - \frac{\partial}{\partial t} \right) R(\vec{r}, t) = \int d^3 r' U(\vec{r}, \vec{r}') R(\vec{r}', t) + O(k^4) = V_{\text{LO}}(\vec{r}) R(\vec{r}, t) + \dots, \quad (2.8)$$

where $t-t_0$ should be moderately large so that states with large k^2 and states with more than 2 particles are suppressed.

For the spin singlet state, we extract the central potential as $V_C(r; J=0) = (\frac{\nabla^2}{2\mu} - \frac{\partial}{\partial t}) R/R$. For the spin triplet state, the wave function is decomposed into the S - and the D -wave components as

$$\begin{cases} R_{\alpha\beta}(\vec{r}; {}^3S_1) = \mathcal{P} R_{\alpha\beta}(\vec{r}; J=1) \equiv \frac{1}{24} \sum_{\mathcal{R} \in O} \mathcal{R} R_{\alpha\beta}(\vec{r}; J=1), \\ R_{\alpha\beta}(\vec{r}; {}^3D_1) = \mathcal{Q} R_{\alpha\beta}(\vec{r}; J=1) \equiv (1 - \mathcal{P}) R_{\alpha\beta}(\vec{r}; J=1). \end{cases} \quad (2.9)$$

Therefore, the Schrödinger equation with the LO potentials for the spin triplet state becomes

$$\begin{Bmatrix} \mathcal{P} \\ \mathcal{Q} \end{Bmatrix} \times \left\{ -\frac{\nabla^2}{2\mu} + V_0(r) + V_\sigma(r) (\vec{\sigma}_\Lambda \cdot \vec{\sigma}_N) + V_T(r) S_{12} \right\} R(\vec{r}, t-t_0) = - \begin{Bmatrix} \mathcal{P} \\ \mathcal{Q} \end{Bmatrix} \times \frac{\partial}{\partial t} R(\vec{r}, t-t_0), \quad (2.10)$$

from which the central and the tensor potentials, $V_C(r; J=0) = V_0(r) - 3V_\sigma(r)$ for $J=0$, $V_C(r; J=1) = V_0(r) + V_\sigma(r)$, and $V_T(r)$ for $J=1$, can be determined.

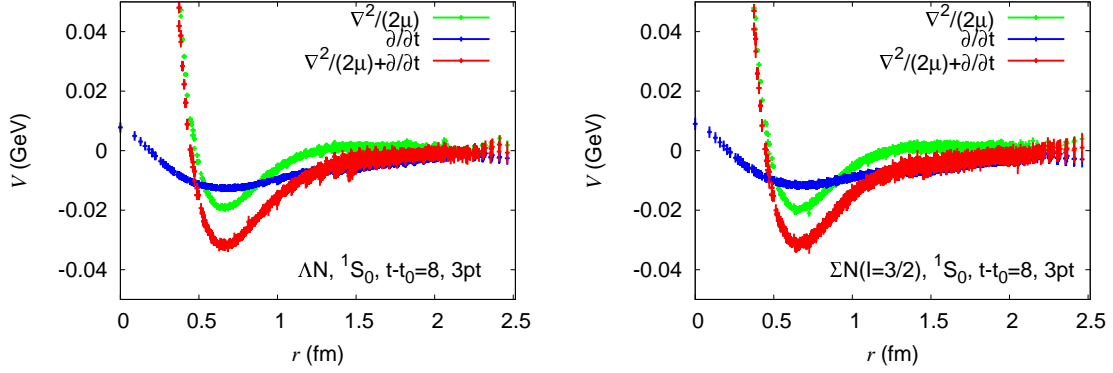


Figure 1: Left: The central potential (red) in the 1S_0 channel of the ΛN system in 2 + 1 flavor QCD as a function of r , together with the $\frac{\nabla^2}{2\mu}$ part (green), $\frac{\partial}{\partial t}$ part (blue). Right: The central potential in the 1S_0 channel of the $\Sigma N(I = 3/2)$ system as a function of r . Symbols are same as the left figure.

3. Numerical simulations

In our calculations for ΛN and $\Sigma N(I = 3/2)$ potentials, we employ 2+1 flavor full QCD gauge configurations generated by PACS-CS collaboration [23] with the RG-improved Iwasaki gauge action and the nonperturbatively $O(a)$ -improved Wilson quark action at $\beta = 1.9$ on a $L^3 \times T = 32^3 \times 64$ lattice. The lattice spacing at the physical quark masses is $a = 0.0907(13)$ fm [23], thus the spatial volume is $(2.90\text{fm})^3$. We have chosen one set of hopping parameters $(\kappa_{ud}, \kappa_s) = (0.13700, 0.13640)$ for light and the strange quarks, which correspond to $(m_\pi, m_K) \cong (699, 787)$ MeV. The wall source with the Coulomb gauge fixing is placed at the time-slice t_0 , and the Dirichlet boundary condition is imposed in the temporal direction at the time-slice $t - t_0 = N_t/2$. A total number of gauge configurations we have used is 399, and we put a source at $t_0 = 8n$ with $n = 0, 1, 2, \dots, 8$ on each configuration to increase the statistics.

4. Results

4.1 ΛN and $\Sigma N(I = 3/2)$ potentials in 1S_0 channel

The ΛN (left panel) and the $\Sigma N(I = 3/2)$ (right panel) potentials in the 1S_0 channel are shown in Figure 1, where the laplacian part is represented by green, the time-derivative part by blue and the total potential by red, respectively. Note that the time derivative term gives a significant attraction at medium and longer distances.

In the 2+1 flavor QCD, while the $\Sigma N(I = 3/2)$ potential still belongs directly to the $\mathbf{27}(I = 3/2)$ representation thanks to the isospin(I) symmetry, an energy eigenstate of a ΛN system in the 1S_0 channel is a mixture of $\mathbf{27}(I = 1/2)$ and $\mathbf{8}_s$ in the flavor representation, so that these two potentials are not necessarily mutually in agreement. As seen from Figure 1, however, these two potentials look very similar to each other, since the flavor symmetry breaking is still small in the present 2 + 1 flavor QCD calculation, where the baryon masses are given by $(m_N, m_\Lambda, m_\Sigma) = (1.574(3), 1.635(3), 1.650(3))$ GeV.

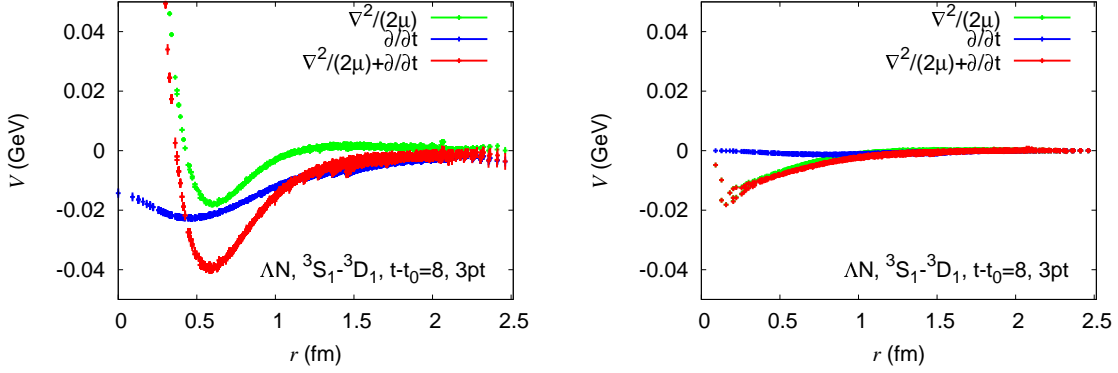


Figure 2: Left: The central potential in the ${}^3S_1 - {}^3D_1$ channel of the ΛN system as a function of r . Symbols are same as the Fig. 1. Right: The tensor potential in the ${}^3S_1 - {}^3D_1$ channel of the ΛN system as a function of r . Symbols are same as Fig. 1.

4.2 ΛN interaction in the ${}^3S_1 - {}^3D_1$ channel

Figure 2 shows the central potential (left panel) and the tensor potential (right panel) of the ΛN system in the ${}^3S_1 - {}^3D_1$ channel, whose eigenstate is a mixture of $\overline{\mathbf{10}}$ and $\mathbf{8}_a$. The time-derivative part (blue) of the central potential has attractive contributions, so that the attraction of the total potential (red) is enhanced at long distance. The attractive well at the distance $r \approx 0.6$ fm is deeper than that of the ΛN central potential in the 1S_0 channel. The time derivative part of the tensor potential, on the other hand, gives a negligible contribution. Furthermore, the tensor potential itself (red) is weaker than the tensor potential of the NN system[18].

4.3 ΣN interaction in the ${}^3S_1 - {}^3D_1$ channel

Figure 3 shows the central potential (left panel) and the tensor potential (right panel) of the $\Sigma N(I = 3/2)$ system in the ${}^3S_1 - {}^3D_1$ channel. Due to the isospin symmetry, this channel belongs solely to the flavor $\mathbf{10}$ representation without mixing with $\overline{\mathbf{10}}$ or $\mathbf{8}_a$.

As seen from an enlargement in the inset of the left panel, there is no clear attractive well in the central potential (red). An attractive well seen in the laplacian part (green) at medium distances is cancelled by a repulsive contribution in the time-derivative part (blue) at the whole range. This repulsive nature of the $\Sigma N(I = 3/2, {}^3S_1 - {}^3D_1)$ central potential is consistent with the prediction from the naive quark model.[24] The tensor force is a little stronger than that of the ΛN system but is still weaker in magnitude than that of the NN system. The time-derivative part gives a negligible contribution.

5. Summary

We have calculated the central and the tensor parts of the ΛN and $\Sigma N(I = 3/2)$ potentials using the improved method. Two potentials in the 1S_0 channel, one is ΛN and another is $\Sigma N(I = 3/2)$, are very similar to each other, since both sectors have a common $\mathbf{27}$ representation in the flavor $SU(3)$ and the $SU(3)$ breaking effect is still small in the present calculation. Both potentials have an attractive well, so that they give attractive interactions at low energy.

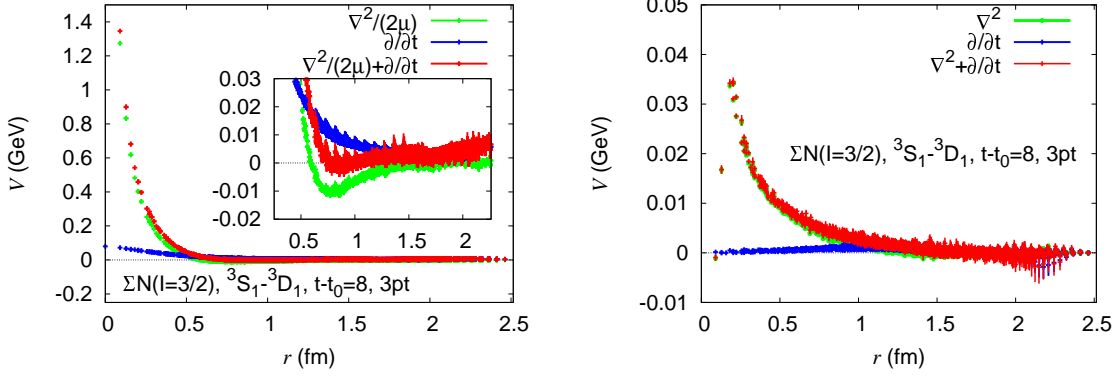


Figure 3: Left: The central potential in the ${}^3S_1 - {}^3D_1$ channel of the ΣN system as a function of r . Right: The tensor potential in the ${}^3S_1 - {}^3D_1$ channel of the ΣN system as a function of r .

In the ${}^3S_1 - {}^3D_1$ channel, while the central ΛN potential shows attraction at low energy with an attractive well, the central $\Sigma N(I = 3/2)$ potential is repulsive at all distances. Tensor potentials for both ΛN and $\Sigma N(I = 3/2)$ systems in this work are rather weak.

In this report, we have extracted single-channel potentials only without coupled-channel analysis between ΛN and ΣN . though the coupled-channel potentials can be also extracted in principle[12, 13]. The author had postponed such a coupled-channel analysis to future publications, since he had to spend his time to recover in various parts of his life and research environment from the massive earthquake in East of Japan on March 11th, 2011. Further analyses including coupled-channel potentials are now in progress.

Acknowledgments

The author would like to thank CP-PACS/JLQCD collaborations, PACS-CS Collaboration and ILDG/JLDG[21] for allowing us to access the full QCD gauge configurations, and Dr. T. Izubuchi for providing a sample FFT code. The author also thank maintainers of C++[25]. Calculations in this report have been performed by using the Blue Gene/L computer under the ‘‘Large scale simulation program’’ at KEK (No. 10-24). He would also like to thank Dr. S. Ejiri, Dr. K. Itahashi and Advanced Meson Science Laboratory of RIKEN Nishina Center for providing a special computer resource, and Prof. H. Tamura and Dr. T. Koike for generous support in recovering the research environment after the massive earthquake in East of Japan on Math 11th. The author is supported by the Global COE Program for Young Researchers at Tohoku University. This research was supported in part by Strategic Program for Innovative Research (SPIRE), the MEXT Grant-in-Aid, Scientific Research on Innovative Areas (Nos. 21105515, 20105003).

References

- [1] Reviewed in O. Hashimoto and H. Tamura, Prog. Part. Nucl. Phys. **57**, 564 (2006).
- [2] H. Nemura, Y. Akaiishi and Y. Suzuki, Phys. Rev. Lett. **89**, 142504 (2002) [arXiv:nucl-th/0203013].
- [3] See e.g. J. Schaffner-Bielich, Nucl. Phys. A **804**, 309 (2008) [arXiv:0801.3791 [astro-ph]].

- [4] P. B. Demorest, *et al.*, Nature **467**, 1081 (2010).
- [5] N. Ishii, S. Aoki, T. Hatsuda, Phys. Rev. Lett. **99**, 022001 (2007).
- [6] S. Aoki, T. Hatsuda and N. Ishii, Prog. Theor. Phys. **123** (2010) 89.
- [7] K. Murano, N. Ishii, S. Aoki and T. Hatsuda, Prog. Theor. Phys. **125** (2011) 1225.
- [8] H.Nemura, N.Ishii, S.Aoki and T.Hatsuda, Phys. Lett. B **673**, 136 (2009).
- [9] T. Inoue *et al.* [HAL QCD collaboration], Prog. Theor. Phys. **124** (2010) 591.
- [10] T. Inoue *et al.* [HAL QCD Collaboration], Phys. Rev. Lett. **106** (2011) 162002.
- [11] T. Doi *et al.*, [HAL QCD Collaboration], arXiv:1106.2276 [hep-lat].
- [12] S. Aoki *et al.* [HAL QCD Collaboration], Proc. Jpn. Acad. B **87**, 509 (2011) [arXiv:1106.2281 [hep-lat]].
- [13] K. Sasaki for HAL QCD Collaboration, in these proceedings.
- [14] Y. Ikeda [for HAL QCD Collaboration], arXiv:1111.2663 [hep-lat].
- [15] Y. Ikeda and H. Iida, arXiv:1102.2097 [hep-lat].
- [16] H. Nemura, N. Ishii, S. Aoki and T. Hatsuda [PACS-CS Collaboration], PoS **LATTICE2008**, 156 (2008) [arXiv:0902.1251 [hep-lat]].
- [17] H. Nemura [HAL QCD Collaboration and PACS-CS Collaboration], PoS **LAT2009**, 152 (2009) [arXiv:1005.5352 [hep-lat]].
- [18] N. Ishii for HAL QCD collaboration, in these proceedings.
- [19] R. Tamagaki and W. Watari, Prog. Theor. Phys. Suppl. **39**, 23 (1967).
- [20] S. Okubo and R.E. Marshak, Ann. Phys. (NY) **4**, 166 (1958).
- [21] See <http://www.lqcd.org/ildg> and <http://www.jldg.org>
- [22] T. Ishikawa *et al.* [CP-PACS/JLQCD Collaboration], Phys. Rev. D **78** (2008) 011502(R).
- [23] S. Aoki *et al.* [PACS-CS Collaboration], Phys.Rev.D79, 034503 (2009) [arXiv:0807.1661 [hep-lat]].
- [24] M. Oka, K. Shimizu and K. Yazaki, Prog. Theor. Phys. Suppl. **137**, 1 (2000).
- [25] Columbia Physics System (CPS), <http://qcdoc.phys.columbia.edu/cps.html>.